Materials Characterization 106 (2015) 266–272

Contents lists available at ScienceDirect

Materials Characterization

journal homepage: www.elsevier.com/locate/matchar

Microstructural evolution and creep-rupture life estimation of high-Cr martensitic heat-resistant steels

Kyu-Ho Lee [a], Jin-Yoo Suh [b], Sung-Min Hong [b], Joo-Youl Huh [c], Woo-Sang Jung [b,*]

[a] Special Steel Development Team, Hyundai Steel, Chungnam 343-823, Republic of Korea
[b] High Temperature Energy Materials Research Center, Korea Institute of Science and Technology, Seoul 136-791, Republic of Korea
[c] Department of Materials Science and Engineering, Korea University, Seoul 136-713, Republic of Korea

ARTICLE INFO

Article history:
Received 13 February 2015
Received in revised form 2 June 2015
Accepted 7 June 2015
Available online 10 June 2015

Keywords:
Heat-resistant steels
Precipitation
Z-phase
Creep-rupture life
Monkman–Grant equation

ABSTRACT

The creep behavior of high-Cr martensitic heat-resistant steels was investigated to discuss the dominant factors determining the creep-rupture life in the temperature range from 839 to 894 K. Variation in the content of Nb, a carbide former, induced a difference in creep-degradation at the long-term creep condition, which was attributed to the formation of a Z-phase at the expense of M_2N precipitates. Due to the continuous evolution of the microstructure during creep service, a simple form of the Monkman–Grant equation could not properly describe the creep-rupture life of the alloys; however, the modified Monkman–Grant equation, which incorporates the creep rate at the tertiary creep region, resulted in a reasonable estimation of creep-rupture life.
© 2015 Elsevier Inc. All rights reserved.

1. Introduction

9–12% Cr martensitic heat-resistant steel is characterized by its superior resistance to oxidation, corrosion, and creep deformation. In addition, the steels are characterized by superior thermo-fatigue resistance compared to that of austenitic heat-resistant steel and a low thermal expansion coefficient. For these reasons, the 9–12% Cr martensitic heat-resistant steels have been constituting the critical parts withstanding hot pressurized steams in the boiler unit of current coal-fired power plants [1–3]. These days, we are facing a significant threat to human society imposed by the limited natural resources and the surge of greenhouse gas emission. To cope with the current situation, not only the development of novel energy resources but also the increase in the efficiency of current power generation, such as coal-fired power generation, is highly required. A foremost requirement for improving power generation efficiency in coal-fired power plants is to increase the operating temperature and steam pressure [3–5]. Thus, the development of materials that can be used in higher temperatures and pressure conditions for a longer time is demanded. As a result, research and development on heat-resistant steel with a superior high-temperature creep property is actively underway [1–8]. An efficient method that improves high-temperature creep properties is to utilize precipitation strengthening. In this context, a number of studies have been conducted on the formation of MX (M = Ti, V, Nb, Ta etc./X = C, N) carbonitride, which is stable at high-temperatures, by adding transition elements such as Ti, V, Nb, and Ta [8]. For the requirements a candidate heat-resistant steel has to meet, ASME Section II defines the following standards regarding the allowable stress values of coal-fired power plants below 1088 K: (1) 100% of the average stress to produce a creep rate of 0.01% in 1000 h ($=10^{-5}$%/h), and (2) 80% of the minimum stress and 67% of average stress to cause rupture at 100,000 h [9]. However, it is not practical to perform a creep test for about 11.4 years (100,000 h). Thus, the traditional estimation of creep strength at 100,000 h has been done by extrapolating from experimental results of less than 30,000 h by making various temperature and stress conditions [7]. Typical estimation methods of creep-rupture life include, (1) a Larson–Miller plot [10,11] based on variables of time and temperature, and (2) a Monkman–Grant plot [12], in which creep-rupture life does not correlate with temperature but is inversely proportional to

Table 1
Chemical composition of high-Cr martensitic heat-resistant steels used in this study (wt.%).

Alloy	Fe	C	Si	Mn	Ni	Cr	Mo	V	W	Cu	Nb	N
Steel A	Bal.	0.18	0.23	0.69	0.52	10.9	0.98	0.20	0.16	0.03	0.06	0.072
Steel B	Bal.	0.16	0.25	0.56	0.35	10.4	0.86	0.17	–	0.13	0.38	0.061

* Corresponding author.
E-mail addresses: kyuhos@hyundai-steel.com (K.-H. Lee), jinyoo@kist.re.kr (J.-Y. Suh), magerit84@gmail.com (S.-M. Hong), jyhuh@korea.ac.kr (J.-Y. Huh), wsjung@kist.re.kr (W.-S. Jung).

http://dx.doi.org/10.1016/j.matchar.2015.06.005
1044-5803/© 2015 Elsevier Inc. All rights reserved.

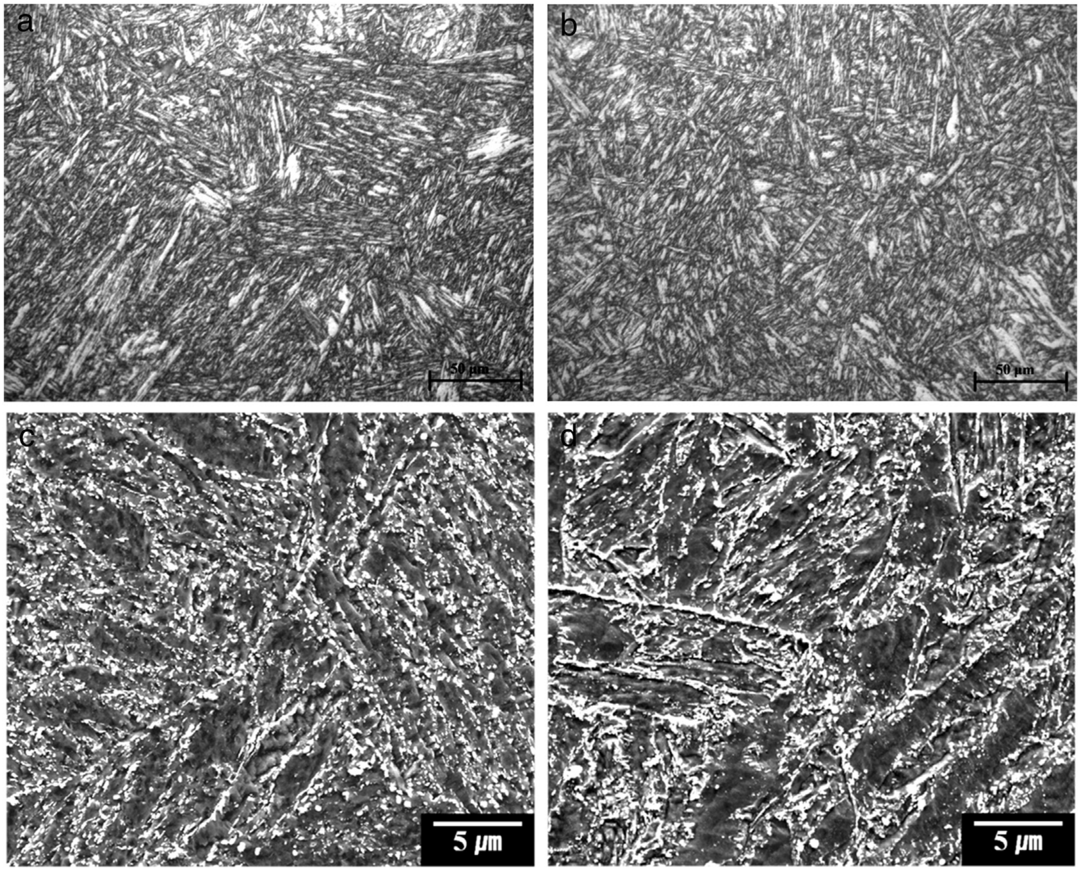

Fig. 1. OM and SEM micrographs of both steels, observed after tempering. OM image of (a) Steel A and (b) Steel B. SEM image of (c) Steel A and (d) Steel B (before creep tests).

the minimum creep rate ($\dot{\varepsilon}_{min}$). They have long been used to estimate the creep-rupture life of many different heat-resistant metals, however it was also reported that the equations were no longer reliable in case of continuous microstructural evolution such as secondary precipitation, coarsening of precipitates, and recrystallization during long-term creep service [13]. Therefore, this study aimed to evaluate the validities of different model equations using the long-term creep data of high-Cr martensitic heat-resistant steels which turned out to have a significant change in creep behavior during long-term creep exposure due to the microstructural evolution. The high-Cr steels were designed to have a different Nb content, which is a strong MX-forming element, to induce a different microstructural evolution among the alloys during creep deformation. Careful observation of the microstructures was carried out to explain the change in creep deformation behavior. Also the creep-rupture life estimated by the model equations was compared with the experimental data.

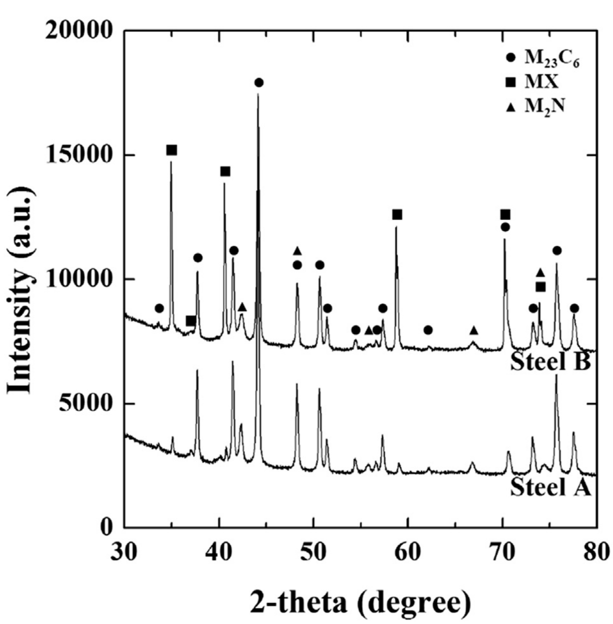

Fig. 2. XRD profiles of the powder electrochemically extracted from Steel A and Steel B after tempering (before creep test).

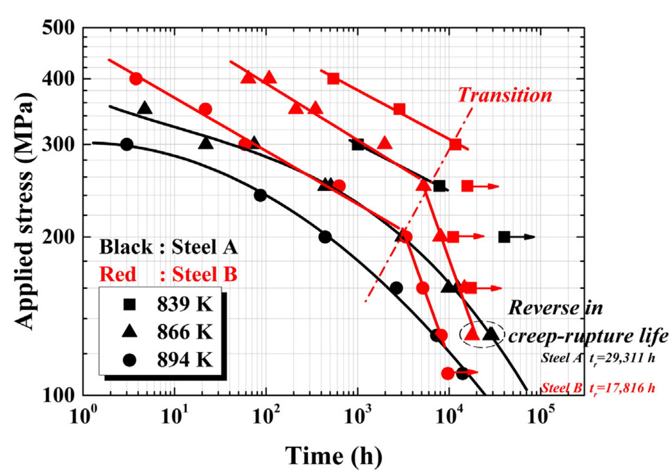

Fig. 3. Creep-rupture properties of Steel A (black symbol) and Steel B (red symbol) acquired through various creep test conditions (the arrow indicates that the creep test for both steels is still ongoing). (For interpretation of the references to color in this figure legend, the reader is referred to the web version of this article.)

Download English Version:

https://daneshyari.com/en/article/7970326

Download Persian Version:

https://daneshyari.com/article/7970326

Daneshyari.com